

Lower-Temperature Electrolyte and Electrode Materials

Dr. Keqin (Kevin) Huang
Siemens Westinghouse Power
Corp.
1310 Beulah Rd.
Pittsburgh, PA 15235-5620

(412) 256-2323
keqin.huang@siemens.com



Lane Wilson
(304) 285-1336
lcwilson@netl.doe.gov

Objectives

- Evaluate state-of-the art electrolyte materials.
- Assess thermodynamic stabilities of perovskite electrolytes.
- Study compatibility of electrodes and electrolytes.
- Study electrochemical polarization behaviors.

Key Milestones

- Complete evaluation of state-of-the art in electrolyte materials by December 2000.
- Complete stability study by September 2001.
- Complete compatibility study by September 2001.
- Complete electrochemical polarization study by September 2002.

Technical Approaches and Results

Extensive literature survey was conducted on electrolyte materials, especially with fluorite and perovskite structures.

Solid Oxide Electrolytes with Fluorite Structure: ZrO_2 -based solid oxide electrolytes are representatives of oxide-ion conductors with fluorite structure. Substitu-

tion of Zr^{4+} with alkaline- and rare- earth cations such as Sr^{2+} , Ca^{2+} , Sc^{3+} and Y^{3+} not only creates a number of mobile oxygen vacancies to achieve appreciable oxide-ion conductivity, but also stabilizes the high-temperature cubic phase. Among those dopants, Sc^{3+} yields the highest conductivity, mainly because of the closest match in ionic radius to Zr^{4+} ($r(Zr^{4+}, VIII) = 0.84 \text{ \AA}$ vs $r(Sc^{3+}, VIII) = 0.87 \text{ \AA}$). Higher conductivity electrolytes are also found in other fluorite-type oxides with larger cations such as CeO_2 and $BiO_{1.5}$. From a structural standpoint, a larger cation tends to be more polarizable, and as a result it increases the mobility of oxide-ions. Among CeO_2 -based electrolytes, Sm-doped CeO_2 exhibits the highest oxide-ion conductivity. However, doped CeO_2 electrolytes are not considered to be practical due to the reduction of Ce^{4+} to Ce^{3+} under a reducing atmosphere, which would induce electronic conduction and dramatic dimensional change.

Solid Oxide Electrolytes with Perovskite

Structure: In 1990, Goodenough et al [1] first pointed out the possibility of high oxide-ion conductivity in perovskites or perovskite-related intergrowth by demonstrating an oxygen vacancy order-disorder transition at 930°C in the brownmillerite compound $Ba_2In_2O_5$. A few years later in 1994, the Sr- and Mg-doped $LaGaO_3$, hereinafter denoted as LSGM, was first reported in both Ishihara's (Japan) and Goodenough's groups (University of Texas at Austin) [2, 3]. The AC conductivity of the LSGM was reported to be 0.10 S/cm at 800°C for the composition of $La_{0.9}Sr_{0.1}Ga_{0.8}Mg_{0.2}O_{2.85}$, and further improved to 0.17 S/cm at the same temperature for the composition of $La_{0.8}Sr_{0.2}Ga_{0.83}Mg_{0.17}O_{2.815}$ after improvement in increasing numbers of oxygen vacancies and phase purity [4, 5]. Soon after its discovery, single SOFCs based on the LSGM were constructed and tested to achieve very encouraging high-power density, even with a thick film ($>500 \mu\text{m}$) [6,7]. Table 1 summarizes the progress on thick-film LSGM-based SOFC achieved in the University of Texas at Austin. It is no doubt that the LSGM electrolyte is a strong candidate for lower temperature SOFCs.

Table 1 Electrochemical Performance of Thick-Film LSGM-Based SOFCs

Years	LSGM electrolyte	Air-electrode/fuel-electrode	V _{cell} (V)@800°C J=300mA/cm ²	MPD@800°C (mW/cm ²)
1995-97	La _{0.9} Sr _{0.1} Ga _{0.8} Mg _{0.2} O _{2.85} L= 500 μm	LSCo40/SDC20+NiO	0.75	270
1998	La _{0.8} Sr _{0.2} Ga _{0.83} Mg _{0.17} O _{2.815} L= 500 μm	LSCo40/SDC20+NiO LSCo40/SDC20/SDC20+NiO	0.85 0.90	440 550
1999	La _{0.8} Sr _{0.2} Ga _{0.83} Mg _{0.17} O _{2.815} L= 550 μm	SCF/SDC20+NiO	0.97	700
2000	La _{0.8} Sr _{0.2} Ga _{0.83} Mg _{0.17} O _{2.815} L= 600 μm	SCF/LDC40+NiO SCF/LDC40/LDC40+NiO	0.98 1.00	800 900

Notes: LSCo40=La_{0.6}Sr_{0.4}CoO_{3-δ}; SDC20= Ce_{0.8}Sm_{0.2}O_{1.9}; SCF= SrCo_{0.8}Fe_{0.2}O_{3-δ}; LDC40= Ce_{0.6}La_{0.4}O_{1.8}

Table 2 Property Comparisons between LSGM and YSZ Electrolytes

	LSGM	YSZ
Crystal Structure	Primitive cubic	Face centered cubic
AC Conductivity	0.17 S/cm @ 800°C	0.12 S/cm @ 1000°C
Ionic transport number	t _{ion} = 1.0	t _{ion} = 1.0
Mechanical properties	Hardness(Gpa)=7.8±0.4 Elastic modulus (Gpa)=187 Poisson's ratio = 0.29 Fracture Toughness (Mpa·m ^{1/2}) =1.11±0.10	Hardness(Gpa)= 12 Elastic modulus (Gpa)= 200 - Fracture Toughness (Mpa·m ^{1/2}) = 11
Chemical stability in CO ₂ -containing atmosphere	Excellent	Excellent
Chemical compatibility at air-electrode interface	Excellent, no chemical reactions occurred	Poor, the La ₂ Zr ₂ O ₇ phase commonly formed
Chemical compatibility at fuel-electrode interface	Poor, La-diffusion, Ga/Mn interdiffusion occurred	Excellent, no chemical reaction occurred

As a summary, some important properties of LSGM and YSZ are compared in Table 2. In addition to much higher oxide-ion conductivity than that of YSZ, LSGM has an excellent chemical and structural compatibility with most of the perovskite air-electrode materials, particularly mixed conductors. This advantage offers the possibility of co-sintering a thin-film LSGM on a cathode substrate.

Assessment of Thermodynamic Stability of Perovskite Electrolytes: The carbonate formation of an alkaline-earth element in a perovskite oxide is a well-known concern and is thermodynamically and structurally favorable at lower temperatures and high CO₂ atmospheres. Practically, carbonate formation could be

detrimental for SOFC applications, since the presence of carbonates on the surface of functional materials considerably deteriorates their electrical conductivity and mechanical stability. A thorough understanding of this process is, therefore, technically important in order to prevent it from occurring in a SOFC generator.

Two approaches have been used to experimentally study the thermodynamic stability of LSGM in CO₂-containing atmospheres—molten salt method and thermal analysis. In the molten salt study, a total of three salt systems were selected, namely KCl-LiCl (T_m=355°C), NaCl-KCl (T_m=658°C) and Na₂CO₃-K₂CO₃ (T_m=650°C), to mix with LSGM powders at a given ratio, followed by annealing the mixture at 450-

800°C for various time in atmospheres of dry air, 6% H_2O +air, 3% CO_2 + N_2 and 6% H_2O +2.8% CO_2 + N_2 . Extensive reactions were found between the electrolyte LSGM and solvent KCl-LiCl at 450°C, regardless of what atmosphere was used. This finding suggests that the salt KCl-LiCl is not suitable for the thermodynamic study on LSGM. On the other hand, no reactions were found between the Na- and K- containing salts and LSGM. In addition, no carbonate formation was found in all CO_2 -containing atmospheres at 800°C, indicating good stability of LSGM in these atmospheres. In thermal analysis study, the weight changes were recorded as a function of time at 800°C and in CO_2 -containing atmospheres. Figure 1 shows the isothermal weight changes of LSGM pellet as a function of time in different CO_2 -containing atmospheres. No weight gains up to 3% CO_2 were observed, which agrees with the theoretical calculations. Appreciable weight gains were only seen when a gas containing CO_2 content greater than 33% was introduced into the furnace. However, the absolute weight gains were found to be much smaller than those predicted (0.002% vs 13.5% for 33% CO_2) by assuming carbonation of lanthanum and strontium in LSGM. The dramatic difference implies the kinetics of the carbonation process are effectively limited at the sample surface due to a well-sintered dense ceramic body (> 99% of the theoretical density). Also observed in Figure 1 is that the carbonation process is kinetically reversible upon CO_2 changes. Whether the formation of this thin layer of carbonates affects the electrical performance of a cell is subject to the cell testing. However, it is worth mentioning that there is no visual difference in the sample before and after TGA measurement.

Electrical Conductivity and Thermal Expansion Coefficient of Bulk LSGM: Electrical conductivity of a well-sintered bar sample (>99% of XRD density) was measured from 500 to 900°C in air and $N_2+3.9\%H_2+3\%H_2O$ atmospheres using 4-probe technique. As expected, a much higher conductivity than that of YSZ was found, and the conductivity remained unchanged in both air and $N_2+3.9\%H_2+3\%H_2O$ atmospheres. The thermal expansion coefficient of the same batch sample was measured with a dilatometer from 25 to 1000°C in air and $N_2+3.9\%H_2+3\%H_2O$ atmospheres. The results are summarized in Table 3. As shown in the table, LSM exhibits a very close thermal expansion match with LSGM. These results suggest that LSM be considered a better cathode material used for the LSGM electrolyte. In addition, the thermal expansion coefficient of LSGM remained unchanged in oxidizing and reducing atmospheres.

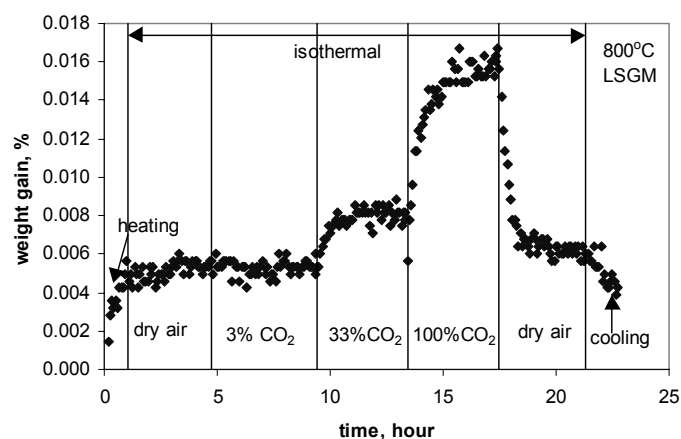
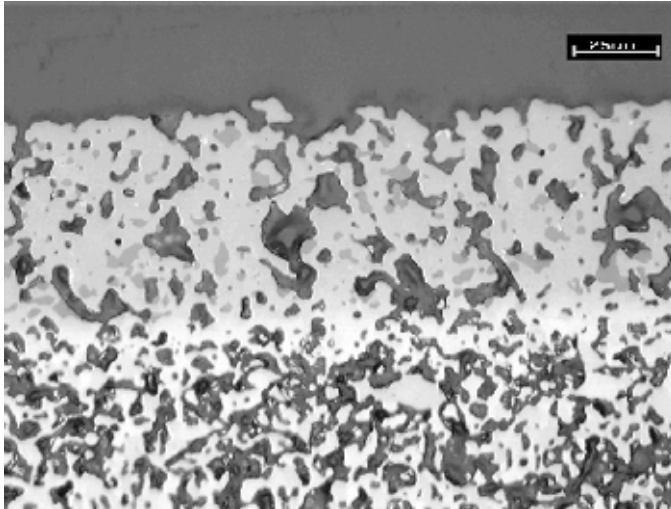


Figure 1. Isothermal weight changes of LSGM at different CO_2 atmospheres

Table 3 Comparisons between LSGM and LSM

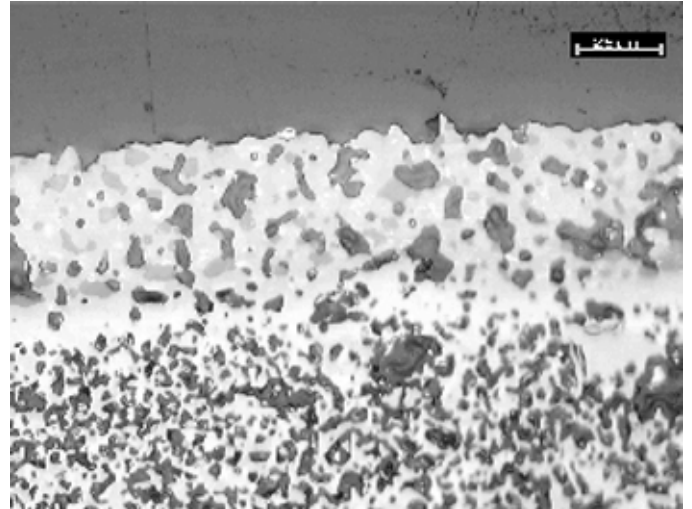
	In air		In $N_2+3.9\%H_2+3\%H_2O$		XRD Structure
	TEC $\times 10^6/K$ (25 - 1200°C)	DC σ at 800°C	TEC $\times 10^6/K$ (25 - 1200°C)	DC σ at 800°C	
LSGM	11.71	0.12 S/cm	11.71	0.12 S/cm	Primitive cubic
LSM	11.71	180 S/cm	-	-	Orthorhombic
LSGM+LSM (1:1 vol%)	11.69	-	-	-	Two-phase mixture

Fully sintered standard WPC3 substrate

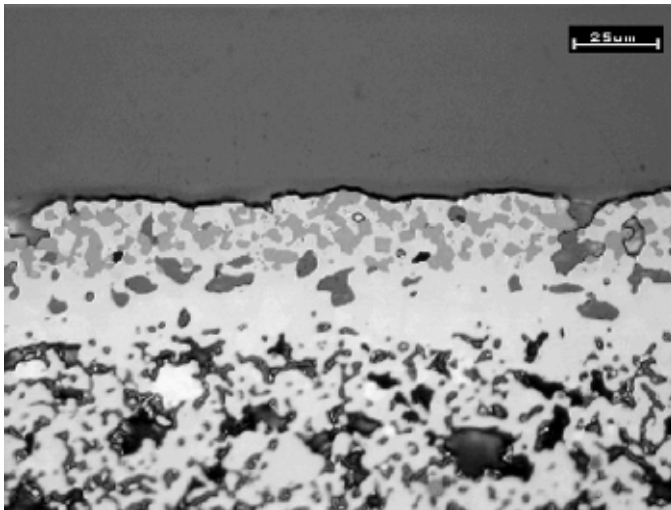


(a) 1450°C

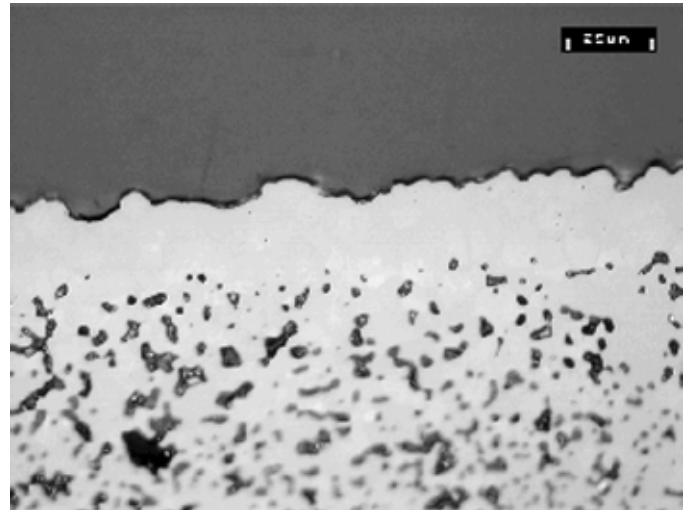
Bisque fired, fine-grained WPC3 substrate



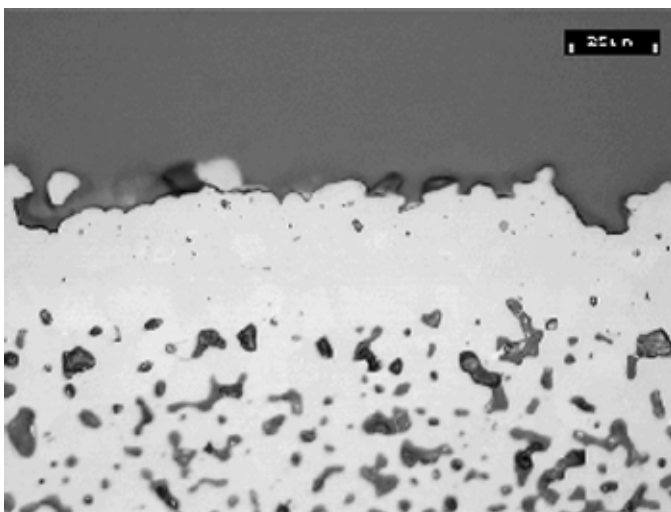
(b) 1450°C



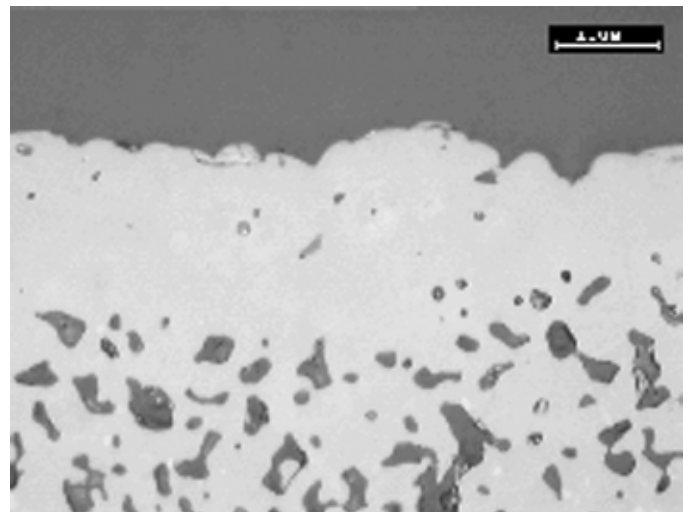
(c) 1475°C



(d) 1475°C



(e) 1500°C



(f) 1500°C

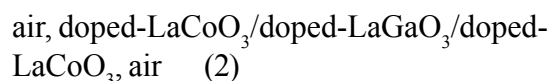
Figure 2. Microstructures of sintered LSGM electrolyte on WPC3 substrates

Co-Sintering of LSGM Thin-Film on the Cathode Substrate: Co-sintering behavior of LSGM film on SWPC proprietary WPC3 cathode substrates were studied. A slurry-coating technique was used to deposit the LSGM film on the porous substrates. The sintering temperatures were chosen from 1450 to 1500°C, each for 3 hours. The window-leak rate of the electrolyte after sintering was subsequently measured, and the microstructure was examined under an optical microscope. It is evident that bisque-fired WPC3 tubes with fine grain size allow more densification of LSGM films than fully sintered tubes with standard grain size. This seems to indicate that the co-shrinkage rate between the film and the substrate determines the densification of the electrolyte film. Microstructural examinations in Figure. 2 showed evolution of microstructure with temperatures and substrates, and agreed well with the window leak-rate results.

Electrochemical Polarization Study: In a fuel cell, the cell voltage V_{cell} is determined by the equation,

$$V_{\text{cell}} = V_{\text{Nernst}} - j(\text{ASR}) - \Sigma\eta \quad (1)$$

where V_{Nernst} is the Nernst potential, V , j is the current density, A/cm^2 , ASR is the ohmic area specific resistance of the cell, $\Omega \cdot \text{cm}^2$, and $\Sigma\eta$ is the sum of all polarization losses in the cell. At low current density, activation polarization represents a large fraction of the total voltage losses in the cell. At moderate current density, the slope of the curve represents the main effect of the ohmic loss, $j(\text{ASR})$. At high current density, the cell voltage is limited by transport of gaseous species reaching and leaving the reaction sites. Polarization is of two kinds: concentration polarization that refers to gas diffusion through the pores in the electrodes, and activation polarization that refers to the charge transfer reaction in the electrodes and at their interfaces with the electrolyte. Both of these phenomena can be conveniently studied by DC-polarization and AC impedance measurements of a cell consisting of the electrolyte membrane sandwiched between two identical electrodes. One of examples of such a cell is



The AC impedance spectrum was measured in the frequency range from 1 mHz to 65 kHz with an AC amplitude of 10 mV. The high frequency intercept on the real axis represents the ohmic resistance associated with cell Configuration (2). The arc portion between low and high frequency reflects the electrode resistance, or so-called polarization resistance. As the thickness of the electrode in Configuration (2) is very small, the aforementioned gas diffusion polarization can be ignored. Therefore, the polarization resistance should predominantly represent the activation polarization or charge-transfer resistance. The electrode resistance of doped LaCoO_3 was found to be much smaller than that of doped LaMnO_3 and showed a strong temperature dependence. It is believed that the mixed conductivity in doped LaCoO_3 plays a critical role in reducing the polarization resistance. In future studies, increasing mixed conductivity of the cathode will be a focus.

Conclusions

A new perovskite-type oxide-ion conductor, Sr- and Mg-doped LaGaO_3 (LSGM), has been selected as a potential electrolyte for low temperature SOFCs, based on an extensive literature survey. The rationale for this selection relies on higher oxide-ion conductivity and better chemical and structural compatibility with electrode substrate exhibited by LSGM in a comparison to YSZ. The assessment on thermodynamic stability of LSGM in CO_2 -containing atmospheres was conducted using both molten-salt and TGA techniques. The results clearly showed that the carbonate formation of LSGM in contact with high concentration CO_2 atmosphere is thermodynamically likely, but kinetically limited to the surface of dense ceramics and negligible overall. Thermal expansion coefficient measurements suggested LSGM have the closest thermal match to Sr-doped LaMnO_3 . LSGM films were fabricated on WPC3 cathode-substrates using slurry-coating technique followed by co-sintering. The chemical compatibility between LSGM films and WPC3 cathode-substrates was then studied on the fabricated couples using an EBMA technique. Although a dense LSGM film is achievable by sintering at a temperature greater than 1450°C, the chemical interdiffusion between Ga and Mn was severe and considerably changed the chemistry of the electrolyte. Lowering the sintering temperature of

LSGM film has been identified as one of the effective ways to alleviate the observed interdiffusion in future.

In future, in addition to further and better understand the observed Ga-Mn interdiffusion, the research will be focused on lowering sintering temperature of LSGM film using a new deposition technique, such as plasma spray.

References

1. J. B. Goodenough, J. E. Ruitz-Diaz, Y. S. Zhen, *Solid State Ionics*, **44**, 21, (1990).
2. T. Ishihara H. Matsuda, Y. Takita, *J. Am. Chem. Soc.*, **116**, 301, (1994).
3. M. Feng and J. B. Goodenough, *Eur. J. Solid State Inorg. Chem.*, **31**, 663, (1994).
4. K. Huang, R. Tichy, and J. B. Goodenough, *J. Am. Ceram. Soc.*, **81**, 2565, (1998).
5. K. Huang, R. Tichy and J. B. Goodenough, *J. Am. Ceram. Soc.*, **81**, 2581, (1998).
6. K. Huang, R. Tichy and J. B. Goodenough, *J. Am. Ceram. Soc.*, **81**, 2581, (1998).
7. K. Huang, J. Wan and K. B. Goodenough, *J. Electrochem. Soc.*, **148**, (7), A788, (2001).